Vaccinia DNA Topoisomerase I: Evidence Supporting a Free Rotation Mechanism for DNA Supercoil Relaxation†

James T. Stivers*

Center for Advanced Research in Biotechnology of the University of Maryland Biotechnology Institute and National Institute of Standards and Technology, 9600 Gudelsky Drive, Rockville, Maryland 20850

Thomas K. Harris and Albert S. Mildvan

Department of Biological Chemistry, The Johns Hopkins University School of Medicine, 725 North Wolfe Street, Baltimore, Maryland 21205-2185

Received November 21, 1996; Revised Manuscript Received March 3, 1997⊗

ABSTRACT: The *Vaccinia* type I topoisomerase catalyzes site-specific DNA strand cleavage and religation by forming a transient phosphotyrosyl linkage between the DNA and Tyr-274, resulting in the release of DNA supercoils. For type I topoisomerases, two mechanisms have been proposed for supercoil release: (1) a coupled mechanism termed *strand passage*, in which a single supercoil is removed per cleavage/religation cycle, resulting in multiple topoisomer intermediates and late product formation, or (2) an uncoupled mechanism termed *free rotation*, where multiple supercoils are removed per cleavage/religation cycle, resulting in few intermediates and early product formation. To determine the mechanism, single-turnover experiments were done with supercoiled plasmid DNA under conditions in which the topoisomerase cleaves predominantly at a single site per DNA molecule. The concentrations of supercoiled substrate, intermediate topoisomers, and relaxed product *vs* time were measured by fluorescence imaging, and the rate constants for their interconversion were determined by kinetic simulation. Few intermediates and early product formation were observed. From these data, the rate constants for cleavage (0.3 s^{-1}), religation (4 s^{-1}), and the cleavage equilibrium constant on the enzyme (0.075) at 22 °C are in reasonable agreement with those obtained with small oligonucleotide substrates, while the rotation rate of the cleaved DNA strand is fast (∼20 rotations/s). Thus, the average number of supercoils removed for each cleavage event greatly exceeds unity ($\Delta n = 5$) and depends on kinetic competition between religation and supercoil release, establishing a free rotation mechanism. This free rotation mechanism for a type I topoisomerase differs from the strand passage mechanism proposed for the type II enzymes.

The topological state of eukaryotic DNA is altered by two general types of DNA topoisomerase activity. The type I topoisomerases catalyze the ATP-independent reversible cleavage and rejoining of one strand of duplex DNA, with the transient formation of a covalent 3′-phosphotyrosyl intermediate between the DNA and a conserved active site tyrosine (Champoux, 1990). The action of these type I enzymes on circular supercoiled DNA results in the removal of supercoils ("relaxation"), and the appearance of DNA topoisomers differing in linking number by steps of one. In contrast, the dyadic type II enzymes have a pair of active site tyrosyl residues which attack both strands of the DNA duplex and catalyze the ATP-dependent transport of a duplex DNA segment through the break (Lindsley & Wang, 1993; Berger et al., 1996). Type II topoisomerases also relax supercoiled DNA, but the process is distinct from that of the type I enzymes in that the linking number changes in steps of two. Despite the importance of topoisomerase-catalyzed supercoil relaxation in cellular processes such as DNA replication and transcription (Wang, 1991), and as a target for chemotherapeutic agents (Liu & Wang, 1991), little is known about the mechanism of supercoil release, especially for the eukaryotic type I enzymes.

Two general mechanisms have been proposed for supercoil release by type I topoisomerases (Figure 1; Champoux, 1990). The first mechanism envisions an enzyme bridge across the broken DNA and *strand passage* of the uncleaved strand through the gap in the DNA (Figure 1A). The second mechanism involves *free rotation* of the DNA around the uncleaved strand (Figure 1B). The free rotation model has been implicated for the *Vaccinia* enzyme on the basis of (i) the lack of any base preference 3′ to the cleavage site (Shuman & Prescott, 1990), (ii) the observation that 3′ segments of the cleaved strand, two to six nucleotides in length, readily dissociate from the enzyme after the cleavage event (Shuman, 1991), and (iii) the fact that as few as two duplex nucleotides 3′ to the cleavage site are required for cleavage (Shuman, 1992). Similar indirect arguments have been made for other eukaryotic type I topoisomerases, as well (Champoux, 1990; Svejstrup et al., 1990). As

†This work was supported in part by the National Institute for Standards and Technology and National Institutes of Health Grant DK28616 (to A.S.M.). J.T.S. was an American Cancer Society Postdoctoral Fellow during part of this work. T.K.H. was supported by National Institutes of Health Postdoctoral Fellowship GM17514.

* Address correspondence to J. T. Stivers. Phone: 301-738-6264. Fax: 301-738-6255.

⊗ Abstract published in *Advance ACS Abstracts,* April 15, 1997.

S0006-2960(96)02880-2 CCC: $14.00

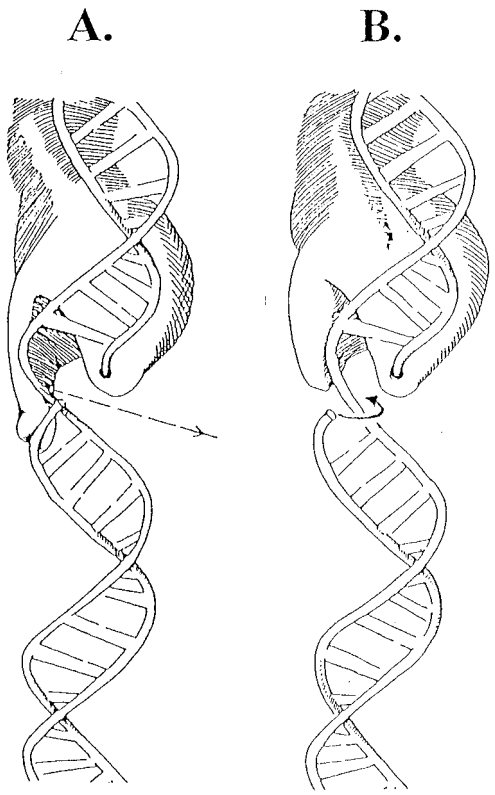

FIGURE 1: Two general mechanisms for relaxation of cleaved supercoiled DNA by type I topoisomerases [modified from Champoux (1990)]. (A) The strand passage mechanism depicts the active transport of the uncleaved DNA strand through the break in the DNA, followed by religation in an obligately coupled cycle of cleavage, strand passage, and religation. In this mechanism, a *single* supercoil is removed for each cleavage event. (B) The strand rotation mechanism depicts the unhindered rotation of the cleaved DNA strand around the axis of the uncleaved strand for removal of supercoils. In this mechanism, *multiple* supercoils would be expected to be removed for each cleavage event.

previously suggested by Champoux (1990), it should be possible to distinguish between these two mechanisms directly by determining how many supercoils are removed for each cleavage/religation cycle.

The *Vaccinia* type I topoisomerase cleaves DNA site-specifically at (C/T)CCTT↓XX sequences (Shuman & Prescott, 1990; Shuman, 1991) and has mechanistic similarities to eukaryotic type I enzymes (Shuman & Moss, 1987; Shuman et al., 1988). Taking advantage of this specificity, we previously determined, using small duplex oligonucleotide substrates, the rate constants for DNA strand cleavage and religation, as well as those for substrate binding and product dissociation (Stivers et al., 1994a). Furthermore, on the basis of the pH dependence and thio effects on these rate constants, general acid−base catalysis and a rate-limiting conformational change for the religation step were suggested (Stivers et al., 1994b). However, these studies on linear substrates could not address the mechanism of supercoil release. In this paper, we address this mechanism directly by studying the relaxation of supercoiled plasmid substrates under single-turnover conditions. A relatively simple kinetic model is employed which describes the reaction in terms of the kinetic partitioning of cleaved supercoiled DNA between religation which forms intermediate topoisomers and supercoil release which forms fully relaxed products. The results we obtain using this approach show that the average number of supercoils released per cleavage/religation event on the enzyme is much greater than unity, consistent with a free rotation mechanism for supercoil removal. The mechanism of super- coil release determined here for a type I enzyme is compared with the proposed mechanism for the type II topoisomerase from yeast (Lindsley & Wang, 1993; Berger et al., 1996).

EXPERIMENTAL PROCEDURES

Materials. The [α-^{32}P]dTTP was from New England Nuclear.[1] The supercoiled pUC19 (2.7 kb) and pHINDF (16.2 kb) plasmid DNAs were isolated from the transformed *Escherichia coli* strain DH5α using a plasmid purification kit (Qiagen). Less than 10% of the final pUC19 DNA and ∼20% of the pHINDF DNA were nicked when using this procedure. An average linking number (ΔLk) for supercoiled pUC19 DNA of 15 was determined by ethidium bromide titration using agarose gel electrophoresis (Keller, 1975; Espejo & Lebowitz, 1976). This average ΔLk corresponds to a superhelix density of −0.056 under these solution conditions (50 mM Tris-HCl, 50 mM NaCl, and 5 mM $MgCl_2$ at pH 7.5 and 22 °C). We estimate, on the basis of this analysis, that ∼90% of the initial pUC19 topoisomer distribution was within two of the average ΔLk (=15). Other reagents were of the highest quality commercially available.

Enzymes. Wild-type *Vaccinia* topoisomerase was over-expressed from *E. coli* strain BL21(DE3) transformed with the T7-based expression plasmid pET21-topo and purified to homogeneity as described (Shuman et al., 1988; Morham & Shuman, 1992). There was no detectable endonuclease activity in this preparation because no time-dependent increase in the amount of nicked circular DNA was observed when the reaction products were analyzed using conditions where nicked DNA was resolved from relaxed closed circular products (a 1% agarose gel containing 1 μg/mL chloroquine was used for this analysis). The concentration of the enzyme was determined by its absorbance at 280 nm (Stivers et al., 1994b) or by the Coomassie dye binding method (Bio-Rad) using bovine serum albumin as the standard. Restriction enzymes and Klenow polymerase were from Life Technologies, Inc.

Single-Turnover Relaxation Kinetics. Single-turnover supercoil relaxation experiments were performed at 22 °C in 50 mM Tris-HCl[2] (pH 7.5), supplemented with 50 mM NaCl and 5 mM $MgCl_2$ using [E]/[DNA] ratios between 1 and 4. These conditions were chosen because the specificity of the enzyme is optimal using these salt concentrations (see Results and Discussion), and the probability of having multiple topoisomerase molecules bound to a single plasmid substrate is minimized at [E]/[DNA] ratios near unity. The reactions were performed in 96-well microtiter plates with V-shaped wells. Reactions were typically initiated by the rapid addition (by manual pipeting) of 10 μL of enzyme (35−375 nM), which had been previously diluted in reaction

[1] Certain commercial equipment, instruments, and materials are identified in this paper in order to specify the experimental procedure. Such identification does not imply recommendation or endorsement by the National Institute of Standards and Technology, nor does it imply that the material or equipment identified is necessarily the best available for the purpose.

[2] Abbreviations: Tris-HCl, tris(hydroxymethyl)aminomethane; SDS, sodium dodecyl sulfate; EDTA, (ethylenedinitrilo)tetraacetic acid, disodium salt.

buffer, to an equal volume of pUC19 DNA (35−190 nM). The reactions were rapidly quenched at various times (1−120 s) by the addition of 10 μL of 10 mass % SDS delivered from a second manual pipetor. For these reactions, accurate quench timing was achieved through the use of a metronome. After quenching, 10 μL of gel-loading buffer consisting of 0.25 vol % bromophenol blue and 30 vol % glycerol in water was added to each sample. The samples (0.3−0.5 μg of DNA/lane) were electrophoresed at 2 V/cm for 18−22 h through a horizontal 1.0 vol % agarose gel in 40 mM Tris-acetate buffer (pH 8.5) containing 1 mM EDTA. The gel was stained in a 500 mL aqueous solution of 0.5 μg/mL ethidium bromide for 15 min and destained for 30 min in 500 mL of deionized water.

To resolve the substrate topoisomers of pUC19, a 1.0 vol % agarose gel containing 25 μg/mL chloroquine diphosphate was used. For this gel, a 40 mM Tris-glycine buffer (50 mM Tris base and 160 mM glycine) containing 1 mM EDTA and 25 μg/mL chloroquine diphosphate was used. Electrophoresis was performed for 20 h at 2.7 V/cm with buffer recirculation. This gel was stained in a 500 mL solution containing 0.5 μg/mL ethidium bromide for 24 h (this was done twice) and then destained in deionized water for 5 h.

Fluorescence intensities were quantitated using an AMBIS fluorescence imager, making appropriate corrections for background fluorescence and the amount of contaminating nicked circles present in the substrates. The fraction of the total fluorescence due to pre-existing nicked circles was determined from the amount of nicked circles present at time zero. This fraction was then subtracted from the total product fluorescence in each lane at subsequent time points. This treatment automatically corrects for sample loading differences between gel lanes.

The combined fluorescence intensities of the supercoiled substrate (F_S) and early topoisomer intermediates that partially overlap with the substrate (F_I) were measured as a unit ($F_{SI} = F_s + F_I$), and the fraction of this fluorescence that was due to unreacted substrate (F_S) was calculated on the basis of the mobility of pure substrate at time zero (r_0), the mobility of the pool of partially resolved topoisomers at infinite time (r_∞), and the mobility of partially overlapped topoisomers at time t (r_t), using eq 1. The fluorescence intensities of the intermediate topoisomers were then calculated by subtracting F_S from F_{SI}.

$$F_S = F_{SI}[1 - (r_t - r_0)/(r_\infty - r_0)] \quad (1)$$

The mobility changes were measured after xerographically enlarging the gel exposures about 4-fold and were well described by a single first-order rate constant indistinguishable from that of strand cleavage (k_{cl}), as would be expected for a sequential series of intermediates with differing mobilities generated from a rate-limiting cleavage event (see Results and Discussion). To confirm this method of calculating the time-dependent change in substrate concentration, the concentration of substrate was also measured directly by resolving substrate topoisomers from all intermediates and product using a 1% agarose gel containing 25 μg/mL chloroquine. In addition to substrate and early intermediates, the fluorescence intensities of late intermediates that were resolved from substrate (F_{I2}) were measured, as well as those of the relaxed product (F_P).

The fractions of substrate, total intermediates, and product present at each time point were then determined by dividing F_S, $F_I + F_{I2}$, and F_P, respectively, by the total fluorescence in each lane ($F_{tot} = F_S + F_I + F_{I2} + F_P$). Control experiments confirmed that the fluorescent signal was linear with respect to DNA concentration in the range of 0.03−0.3 μg ($R^2 = 0.98$) and that there was no significant difference in the fluorescence yield of supercoiled DNA and the relaxed products. Although a higher fluorescence yield would be expected for supercoiled DNA due to its increased capacity for ethidium binding as compared to relaxed closed circular DNA, this effect was not observed due to the unavoidable nicking of the DNA during exposure of the stained gel to UV light prior to quantitation.

Equilibrium DNA Cleavage Measurements. Determinations of the cleavage sites in linearized 3′-^{32}P-labeled pUC19 DNA were performed at 22 °C and pH 7.5 in either 50 mM Tris-HCl buffer or a buffer consisting of 50 mM Tris-HCl, 50 mM NaCl, and 5 mM $MgCl_2$. The 3′ ^{32}P labeling of both strands of pUC19 was achieved by first linearizing the DNA with *Xba*I restriction enzyme and then extending the 3′ ends with Klenow DNA polymerase using [α-^{32}P]TTP and unlabeled NTPs. The DNA was then purified from unincorporated label by batch chromatography using a silica-based resin (Qiagen). Equilibrium cleavage measurements were made by mixing 30 nM end-labeled DNA with increasing concentrations of topoisomerase in the range of 0−750 nM in a volume of 20 μL. After a 15 min incubation, the cleaved enzyme−DNA covalent complex was trapped by the addition of 2 μL of 2 mass % SDS (Stivers et al., 1994a,b). The samples were then adjusted to 40 vol % formamide, heated at 95 °C for 5 min, and cooled on ice, prior to electrophoresis through a prerun 3.0 vol % acrylamide, 7.5 M urea gel prepared in TBE buffer (90 mM Tris-borate and 2.5 mM EDTA) at 400 V for 2 h. The gel was dried, and the labeled DNA was quantitated using a phosphorimager (Fujix BAS 1000).

The *apparent* cleavage equilibrium at each site was determined by measuring the counts in each band and then dividing this by $^1/_2$ of the sum of all the counts in each lane [i.e. K_{cl}^{app} = (cleaved DNA counts)/($^1/_2$ of the total DNA counts)]. Dividing the total DNA counts by a factor of 2 is necessary because the uncleaved 3′-labeled DNA strands comigrate in the gel, and therefore, the specific activity of this band is twice that of the cleaved strands. To obtain the *true* cleavage equilibrium, the apparent equilibrium must be corrected to take into account cleavage at intervening sites between the 3′ label and the site where the cleavage equilibrium is to be determined. Cleavage at these intervening sites reduces the cleaved DNA counts that are measured at sites more distant from the label (i.e. in the 5′ direction). Therefore, the true cleavage equilibrium (K_{cl}) is calculated by dividing K_{cl}^{app} by $1 - \sum K_{cl}^{app}$, where the sum is taken over all sites that intervene between the 3′ label and the site in question (see the cleavage map in Figure 3A).

Theory. A general method for determining the lifetime of an unstable or short-lived intermediate that partitions between kinetic pathways is measurement of the rates of formation of stable intermediates or products that result from this partitioning (Fersht, 1985). Since the relaxation mechanism followed by all type I topoisomerases involves a short-lived covalent phosphotyrosine intermediate, it should be possible, using single-turnover conditions, to measure the

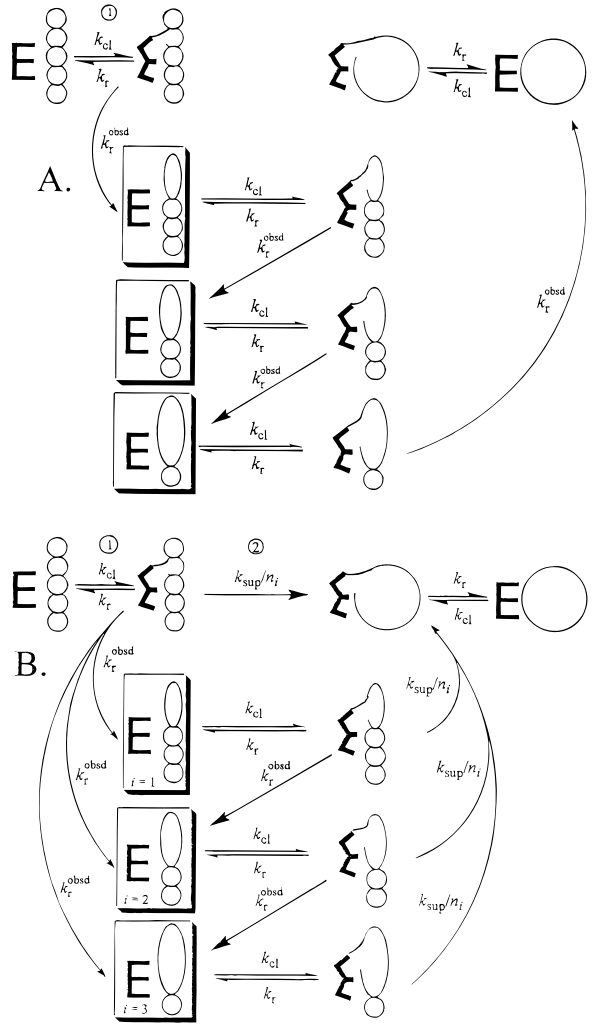

FIGURE 2: Relaxation of enzyme-bound supercoiled DNA by a type I topoisomerase using a strand passage (A) or free rotation mechanism (B). The hypothetical relaxation of a plasmid with four superhelical turns is depicted. For clarity, only the cleaved DNA strand is depicted. A key step regardless of the mechanism involves the reversible formation of a covalent bond between a tyrosine residue of the enzyme and the phosphodiester backbone of the supercoiled DNA molecule (step 1). This step is characterized by the equilibrium constant for cleavage ($K_{cl} = k_{cl}/k_r$) and the two rate constants, k_{cl} and k_r, for cleavage and religation of the DNA, respectively. (A) For a strand passage mechanism, a single supercoil is removed from the initial cleaved supercoiled DNA and a religation event occurs, generating a topoisomer intermediate with ΔLk $-$ 1 supercoils. The cycle of cleavage, removal of a *single* supercoil, and religation is repeated ΔLk times until the DNA molecule is fully relaxed. (B) For a free rotation mechanism, the initial covalent intermediate generated in step 1 may be partitioned between two kinetic pathways. The first pathway, described by the rate constant for relaxation (k_{relax}, step 2), leads to complete unwinding of the DNA and the generation of fully relaxed closed circular product. The second pathway, described by the observed rate constant for religation (k_r^{obsd}, see the text and eq 6), results in the formation of any one of three possible intermediate topoisomers (boxes). These intermediates must be cleaved and again partitioned between relaxation to form product or religation to form another intermediate. Thus, the relative amounts of intermediates and product that are generated at each time point depend on the kinetic competition between the unwinding rate (k_{sup}) and the observed rate of religation (k_r^{obsd}). In this figure, we show the enzyme$-$DNA covalent complex in a different conformational state ("bent" E), as suggested by previous kinetic and biochemical studies (Stivers et al., 1994b; Sekiguchi & Shuman, 1994a,b, 1995, 1996). This model may be extended to supercoiled substrates with a greater number of supercoils, by assuming that partitioning results in the formation of pools of topoisomer intermediates (*i*). Each pool consists of a Boltzmann distribution of topoisomers characterized by an average linking number (see the text).

partitioning of this intermediate between complete unwinding which forms fully relaxed, enzyme-cleaved DNA and religation which forms topoisomer intermediates. This competition between the rate constants for complete unwinding of the DNA, as opposed to religation to form a topoisomer intermediate, provides an internal "clock" that can be used to determine the average number of supercoils removed per cleavage/religation event and, thus, the mechanism of supercoil release. A kinetic treatment for a strand passage and free rotation mechanism using this analytical approach is developed below.

Because, by definition, only one supercoil is removed for each cleavage/religation event in a strand passage mechanism (Figure 2A), a pathway for removal of multiple supercoils does not exist. Therefore, this mechanism is modeled kinetically by assuming that each cleaved supercoiled DNA molecule obligately passes through a sequential series of topoisomer intermediates to reach fully relaxed product (Figure 2A). Because for a strand passage mechanism religation and supercoil release are tightly coupled, the rate constant for supercoil release and religation (k_r^{obsd} in Figure 2A) is a composite rate constant reflecting relaxation of a single supercoil and religation of the DNA strand. A simple indicator for this type of mechanism that distinguishes it from a free rotation mechanism is the fact that many intermediates accumulate before a significant amount of fully relaxed product is formed. This point is demonstrated later in model simulations (see Results and Discussion).

For a free rotation mechanism, the kinetic analysis is more complicated because each cleaved intermediate can freely partition between supercoil release and religation to form one of many topoisomer intermediates (Figure 2B). Consequently, the complete kinetic analysis of the relaxation of a plasmid containing 15 ± 2 supercoils such as pUC19 would require modeling the partitioning of 14 intermediate topoisomers, leading to a kinetic mechanism with greater than 120 steps. Fortunately, the kinetic analysis of DNA relaxation occurring by a free rotation mechanism can be simplified by assuming that partitioning results in the formation of *i* pools of topoisomer intermediates, with the average linking number of each pool differing by Δn supercoils (Figure 2B). These pools of intermediates must be cleaved and partitioned once again to form either relaxed product or new intermediates. A reasonable number of pools (i_{tot}) necessary to model the relaxation reaction for a given substrate is determined by the ratio ΔLk/Δn, that is the total number of supercoils in the substrate (ΔLk) divided by the *average* number of supercoils removed from a cleaved supercoiled intermediate before a religation event occurs (Δn). The kinetic equations describing a free rotation mechanism and a method for estimating i_{tot} and Δn from the kinetic partitioning between supercoil release and strand religation are described below.

As shown in eqs 2 and 3, the observed time constant ($1/k_{relax}$) for the formation of fully relaxed cleaved product (E$-$P) from a cleaved supercoiled intermediate with ΔLk supercoils (E$-S_{\Delta Lk}$) is equal to the time constant for one complete rotation of the cleaved DNA strand ($1/k_{sup}$), multiplied by the number of supercoils (n_i) that had to be removed from the cleaved intermediate to result in fully relaxed product. Because of the reciprocal relationship between time constants and rate constants, eq 3 can also be expressed as shown in eq 4.

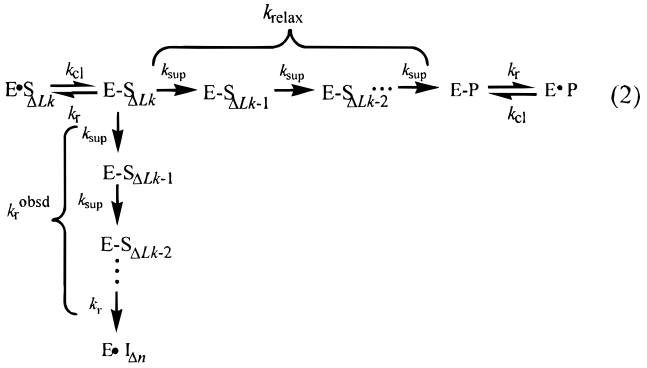

(2)

$$1/k_{relax} = n_i/k_{sup} \quad (3)$$

$$k_{relax} = k_{sup}/n_i \quad (4)$$

Similarly, the average time constant for religation ($1/k_r^{obsd}$, eq 5) for formation of a new distribution of topoisomers with an average of Δn fewer supercoils ($E \cdot I_{\Delta n}$, eq 5) is equal to the microscopic time constant for religation ($1/k_r$, eq 5), plus the net time constant for release of Δn supercoils ($\Delta n/k_{sup}$, eq 5). As with eq 3 above, eq 5 can be equivalently expressed in terms of rate constants (eq 6).

$$1/k_r^{obsd} = \Delta n/k_{sup} + 1/k_r \quad (5)$$

$$k_r^{obsd} = k_{sup}k_r/(\Delta n\, k_r + k_{sup}) \quad (6)$$

As shown in eqs 7 and 8, the value of Δn may be calculated from the ratio of the rate constants k_{sup}/k_r. This simple relationship between the partitioning rate constants and Δn is based on the idea that the *most probable* number of supercoils removed from a cleaved intermediate will be the number that makes the total transit time for removal of supercoils ($\Delta n/k_{sup}$) equal to the microscopic time constant for religation ($1/k_r$).

$$\Delta n/k_{sup} = 1/k_r \quad (7)$$

$$\Delta n = k_{sup}/k_r \quad (8)$$

Once Δn is obtained using eq 8, the total number of intermediate pools (i_{tot}) may then be calculated by dividing the total number of supercoils (ΔLk) by the average number of supercoils removed per cleavage event (Δn) using eq 9.

$$i_{tot} = \Delta Lk/\Delta n \quad (9)$$

The results of model simulations for both a strand passage and free rotation mechanism, and the limitations of the approach outlined above, are discussed in Results and Discussion.

Data Modeling. The changes in concentration of the substrate DNA, all intermediate topoisomers, and products as a function of time were simulated by computer using a modification (Anderson et al., 1988) of the kinetic simulation program KINSIM (Barshop et al., 1983), using the kinetic mechanism shown in Figure 2B. In this analysis, we assume that k_{cl}, k_r, and k_{sup} do not change during relaxation of the DNA. This assumption is reasonable because the values of these constants are similar to those measured with small linear substrates, and the equilibrium constant k_{cl}/k_r calculated from the kinetic data on a supercoiled substrate is similar to that made from equilibrium measurements using linear substrates [see Results and Discussion and Stivers et al. (1994a)]. Moreover, a separate analysis of the rates of appearance and disappearance of early intermediates (i.e. those that were partially overlapped with substrate) and late intermediates (i.e. those that were resolved from substrate) revealed no detectable differences. If a large change in k_{cl}, k_r, and k_{sup} occurred as a result of relaxation of the DNA, it would have been apparent from this analysis. A detailed description of the four-step protocol used to model the relaxation of pUC19 is available as Supporting Information.

We were unable to apply this approach to the larger plasmid pHINDF (~90 supercoils) because of the large number of partitioning intermediates that are generated during relaxation of this plasmid. On the basis of the average number of supercoils released per cleaved intermediate with pUC19 ($\Delta n = 5$), a value of i_{tot} of ~20 (=90/5) for pHINDF would be expected. Moreover, the partitioning of these 20 pools would lead to a kinetic mechanism with greater than 120 steps. Therefore, we do not rigorously quantitate the data for pHINDF but only compare the product to intermediate ratio ([P]/[I]) as a function of time with that measured for pUC19 (see Results and Discussion) to demonstrate that the free rotation mechanism of Figure 2B describes the relaxation of this plasmid as well.

RESULTS AND DISCUSSION

Before single-turnover kinetic experiments were performed on the relaxation of pUC19 supercoiled DNA, which has 17 C/TCCTT consensus cleavage sites (Shuman & Prescott, 1990), it was important to find experimental conditions that favored, *on average*, a single covalent complex per DNA molecule.[3] We approached this problem in two ways. First, we kept the [E]/[DNA] ratio between 1 and 4 for the single-turnover experiments so that, according to Poisson statistics, DNA with more than one enzyme molecule bound would be disfavored. Second, we used high enough concentrations of $MgCl_2$ and NaCl so that weak cleavage sites would be suppressed. As described in the next section, the combined effects of these two approaches abrogated detectable cleavage events at all but two sites in pUC19 for [E]/[DNA] ratios as large as 25.

Equilibrium Strand Cleavage. To ascertain how many sites were cleaved in pUC19 DNA, equilibrium cleavage measurements (Figure 3) were performed by mixing topoisomerase with linearized 3′-^{32}P-labeled pUC19 DNA and trapping the covalent adduct by the rapid addition of SDS (Shuman & Prescott, 1990; Stivers et al., 1994a). Cleavage sites can be located because the protein remains bound in a 3′-phosphotyrosyl linkage to the unlabeled portion of the DNA, and the 3′-labeled portion of the DNA can be detected, and its size determined, using polyacrylamide gel electrophoresis under denaturing conditions.

As shown in Figure 3, six major cleavage sites in the DNA are detected when low salt concentrations are used and the [E]/[DNA] ratio is 25 (lane 3, sites a−f). However, when

[3] Our initial approach was to use a small ~500 bp supercoiled plasmid substrate containing a single *Vaccinia* virus consensus sequence. However, *no topoisomer intermediates were observed* in single-turnover experiments using this plasmid (which contained about four supercoils). This result is expected on the basis of the results presented here with pUC19, which demonstrate that on average five (Δn) supercoils are removed for each cleavage event. Thus, small plasmid substrates with few supercoils are not useful for estimating Δn when a free rotation mechanism is followed.

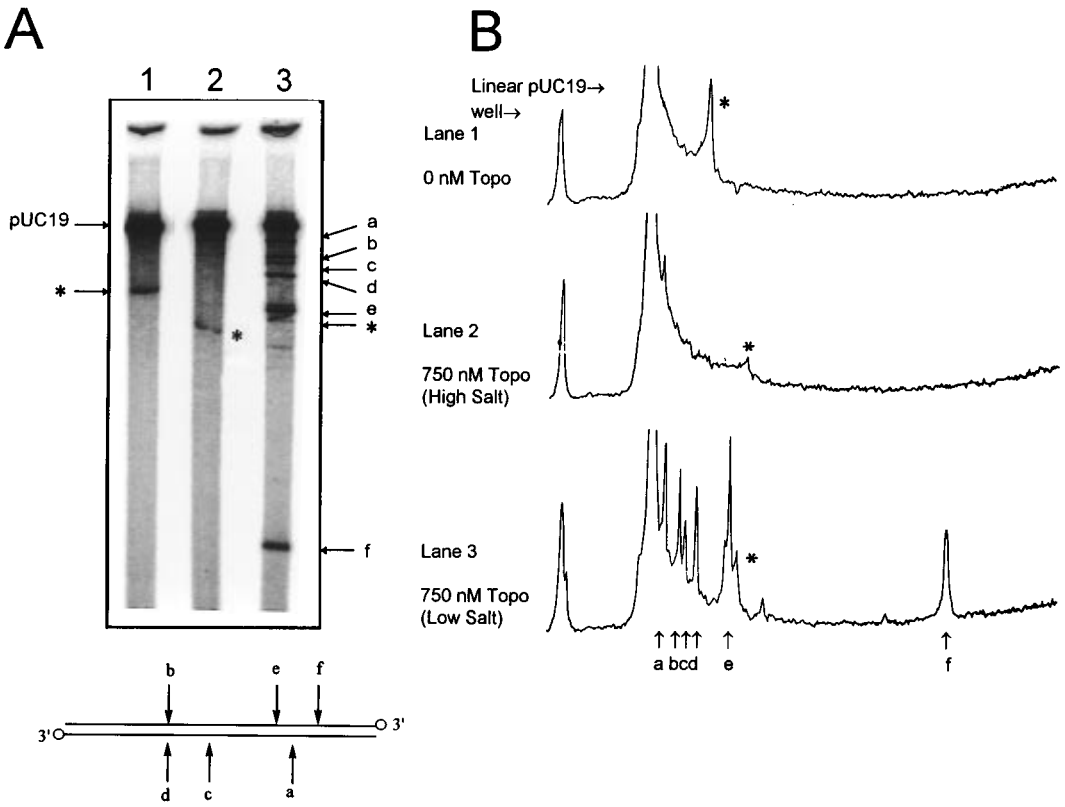

FIGURE 3: Site-specific cleavage by *Vaccinia* topoisomerase in low- and high-ionic strength buffers. 3′-^{32}P-labeled *Xba*-I-cut pUC19 DNA was incubated with purified topoisomerase, treated with SDS, and analyzed by polyacrylamide gel electrophoresis. (A) Phosphorimage of the gel showing cleavage of 30 nM pUC19 catalyzed by 750 nM topoisomerase in either 50 mM Tris-HCl buffer, at pH 7.5 (lane 3) or 50 mM Tris-HCl, supplemented with 50 mM NaCl and 5 mM $MgCl_2$ (lane 2). A control DNA without topoisomerase is shown in lane 1. The band marked with an asterisk in each lane (including the control lane) is due to dsDNA that renatured prior to or during electrophoresis. For reference, the positions of the cleavage sites on each strand of pUC19 DNA are also shown (Shuman & Prescott, 1990). (B) Densitometric traces for each of the lanes shown in panel A. In this gel, the specific activity of the uncleaved DNA band is 2-fold greater than that of the cleaved DNA bands because the uncleaved DNA strands comigrate, and each strand has a 3′ label (see Experimental Procedures). Thus, direct visual comparisons of the fractional extent of cleavage at each site are misleading.

higher salt concentrations are used (Figure 3, lane 2), only one major cleavage site (site a) and a second minor site (site b) are detected when the [E]/[DNA] ratio is 25 [the additional band marked with an asterisk is due to double-stranded (ds) DNA that renatured prior to or during electrophoresis]. Other experiments using these higher salt concentrations demonstrated that no additional cleavage sites were detectable even when a 125-fold greater enzyme concentration was used and that the extent of cleavage at sites a and b did not increase over that shown in Figure 3 (not shown).[4] Taken together, these results show that the specificity of the enzyme is increased at these salt concentrations and that the ratio of cleaved to uncleaved DNA at other individual sites must be $\leq$1%, on the basis of the signal-to-noise ratio of the data in Figure 3B. Thus, at the salt concentrations and comparatively low [E]/[DNA] ratios used in the single-turnover experiments, it is unlikely that a single DNA molecule is cleaved by more than one enzyme molecule. The independence of the kinetic results for [E]/[DNA] ratios in the range of 1−3 also strongly supports this conclusion (see below).

From the ratio of cleaved DNA to uncleaved DNA at site a using the high salt concentrations, an equilibrium constant K_{cl} ($=k_{cl}/k_r$) of 0.08 $\pm$ 0.04 for cleavage of enzyme-bound DNA can be estimated. Similar values for K_{cl} in the range of 0.04−0.10 were calculated for sites a−f using the low salt conditions (the average value for K_{cl} was 0.07 $\pm$ 0.02). This average value for K_{cl} does not differ greatly from the average value of 0.12 $\pm$ 0.02 determined from equilibrium measurements using small oligonucleotide substrates (Stivers et al., 1994a) and those values calculated from kinetic measurements of k_{cl} and k_r, using both supercoiled pUC19 DNA (0.075; see below) and linear DNA (0.08−0.11; Stivers et al., 1994a). Thus, these results indicate that the cleavage equilibrium at the six individual sites differs by less than 40% from the average value of 0.07 for supercoiled pUC19 DNA and that this equilibrium is similar for linear and supercoiled DNA molecules.

Model Simulations. Kinetic simulations for a strand passage and free rotation mechanism for supercoil release from a hypothetical plasmid with four supercoils are shown in panels A and B of Figure 4, respectively. The simulated data points in this figure were generated using KINSIM employing the respective three intermediate models shown in Figure 2A,B. For these model simulations, we chose values for k_{cl} and k_r of 0.3 and 4 s^{-1}, respectively, so that the rate constants and the cleavage equilibrium ($K_{cl} = k_{cl}/k_r$) were the same as the experimentally determined values. For the strand passage mechanism, k_r^{obsd} was set to the same value

[4] Both the number of sites and the salt dependence of the cleavage pattern seen here are similar to those reported by Shuman and Prescott (1990), although somewhat different conditions were used in the previous study (37 °C, 50 mM Tris-HCl with or without 2.5 mM $MgCl_2$ or 150 mM NaCl). Furthermore, these workers mapped the specific cleavage sites at the nucleotide level and demonstrated that the conserved pentamer sequence (C/T)CCTT↓ immediately preceded the site of cleavage in each case.

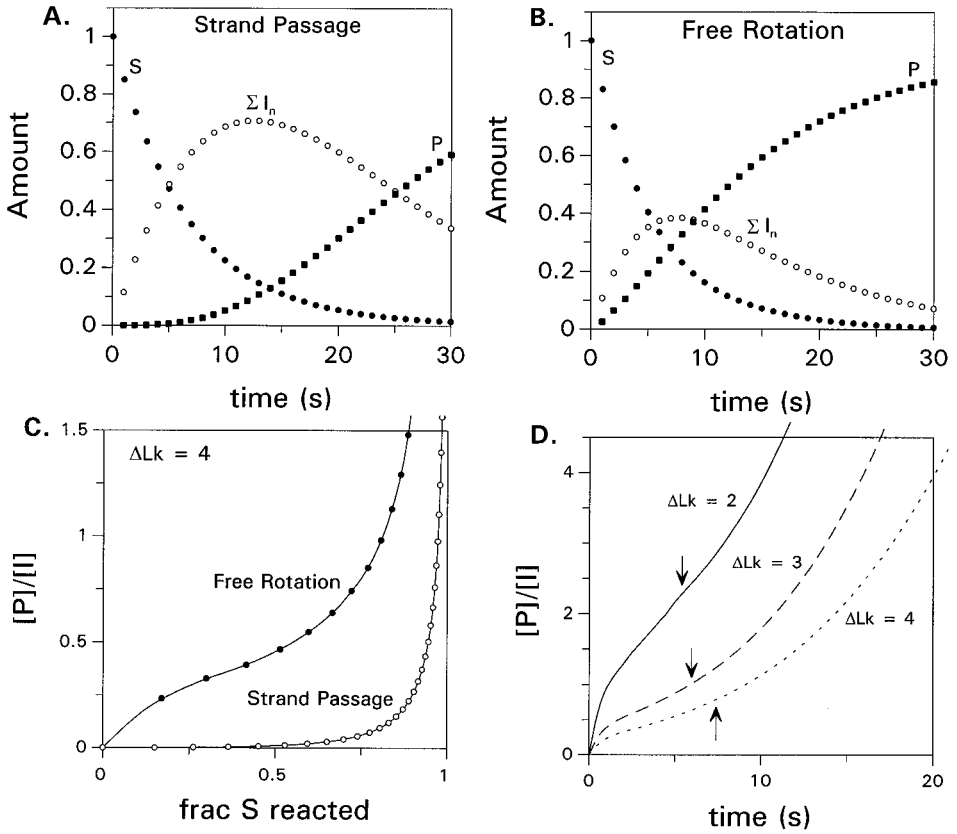

FIGURE 4: Simulated data for the relaxation of a hypothetical plasmid with four (ΔLk) supercoils. (A) Relaxation by a strand passage or (B) free rotation mechanism. We chose values for k_{cl} and k_r of 0.3 and 4 s^{-1}, respectively, so that the rate constants and the cleavage equilibrium ($K_{cl} = k_{cl}/k_r$) are the same as the experimental values (see Results and Discussion). For the strand passage mechanism (Figure 2A), k_r^{obsd} was set to the same value as k_r (4 s^{-1}) because the rate of unwinding a single supercoil cannot be any faster than the rate of religation. For the free rotation mechanism, a value for k_{sup} of 5 s^{-1} was used so that the rate constant for partitioning to product ($k_{relax} = k_{sup}/n_i$) was the same as the experimental data obtained with pUC19. This value of k_{sup} was required because this model assumes a plasmid containing only four supercoils. (C) A plot of the product to intermediate ([P]/[I]) ratio *vs* the fraction of substrate reacted for the simulated free rotation and strand passage data shown in panels A and B. (D) Plot of the [P]/[I] ratio against time for the relaxation of three hypothetical plasmid substrates with differing numbers of supercoils (ΔLk = 2−4). The curves for the plasmids with two and three supercoils were derived from a free rotation mechanism analogous to that shown in Figure 2B. The arrows in panel D correspond to the respective reaction time points where d[I]/dt = 0; the slope of a tangent at these points is inversely proportional to the number of supercoils in the plasmid (see the text).

as k_r (4 s^{-1}) because the net rate of unwinding a single supercoil and religating the cleaved strand cannot be any faster than the rate of religation. For the free rotation mechanism, a normalized value for k_{sup} of 5 s^{-1} was used so that the rate constant for partitioning to product ($k_{relax} = k_{sup}/n_i$) was the same as the experimental data obtained with pUC19.

The strand passage mechanism (Figure 4A) shows the formation of a large pool of intermediates and a pronounced lag before any fully relaxed products appear, while the free rotation mechanism (Figure 4B) shows the parallel formation of intermediates and product. The plot in Figure 4C shows that the product to intermediate ([P]/[I]) ratio *vs* the fraction of substrate reacted differs significantly for the two mechanisms and that they can be easily distinguished under these conditions. In Figure 4D, for a free rotation mechanism, is shown a plot of the product to intermediate ([P]/[I]) ratio *vs* time for three hypothetical plasmids with differing numbers of supercoils (ΔLk = 2, 3, and 4). This plot shows that, for a free rotation mechanism, the rate of product formation when the intermediates are in a steady state (i.e. when d[I]/dt ∼ 0; see the legend to Figure 4D) is inversely proportional to the number of supercoils in the plasmid.

In other modeling studies, it was demonstrated that simulated data (for a plasmid with ΔLk supercoils relaxing by a free rotation mechanism) could be kinetically modeled using only i_{tot} (=ΔLk/Δn) intermediate pools (eq 9). In these modeling studies, the best fit values of k_{cl}, k_r, and k_{sup} differed by less than 10% from the true values used to generate the simulated data. In addition, it was found that using values of i_{tot} less than or significantly greater than the optimal value resulted in an underestimation or overestimation, respectively, of the maximal concentration of the intermediates. Thus, it is possible to model this symmetric and highly repetitive type of reaction using only i_{tot}, and the results are sensitive to this value (eq 9).

Single-Turnover Relaxation Kinetics. Experimental data for the relaxation of pUC19 supercoiled DNA by *Vaccinia* type I topoisomerase show the parallel formation of intermediates and fully relaxed product with essentially no lag (Figure 5A−C). The data closely resemble the simulation of Figure 4B rather than 4A, consistent with a free rotation mechanism for relaxation. The kinetic parameters derived from the data are shown in Table 1. The optimal fit was obtained using the model in Figure 2B, with the number of pools of intermediates (i_{tot}) equal to three and an average number of supercoils removed per cleaved intermediate (Δn) of five. In arriving at these optimal values, we were able to easily exclude a relaxation mechanism involving rapid

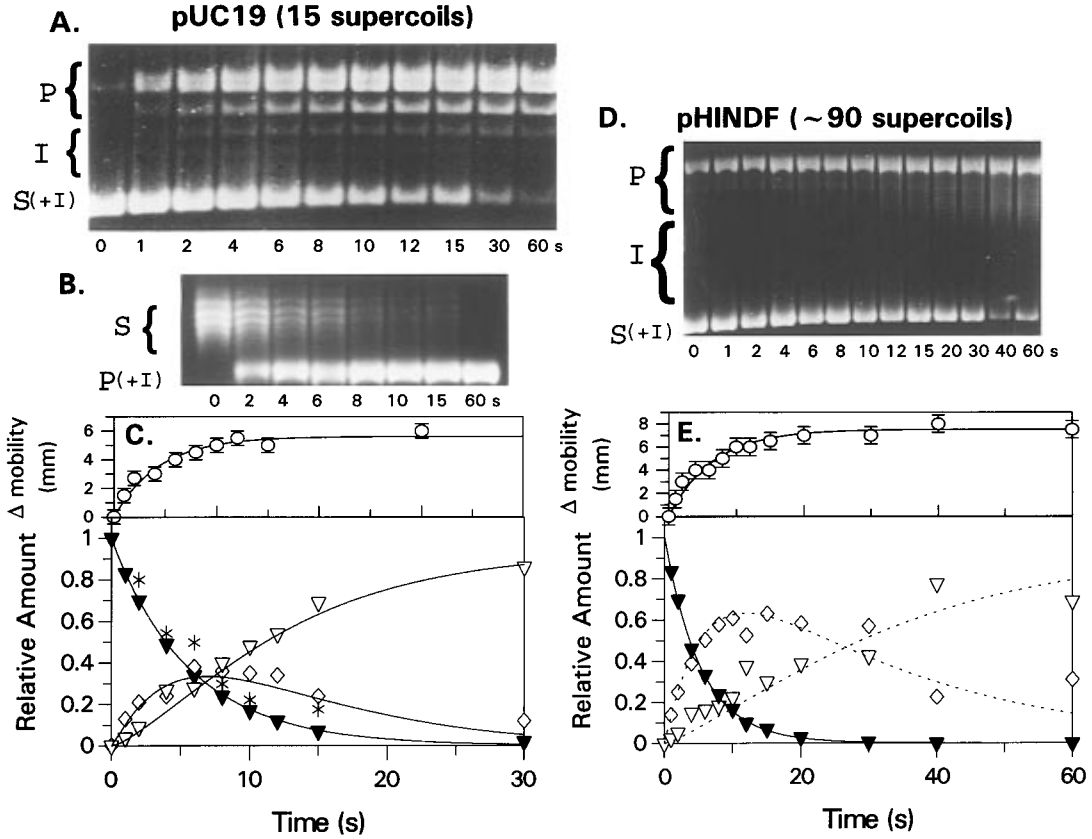

FIGURE 5: Relaxation of supercoiled pUC19 (2.7 kb, 15 supercoils) and pHINDF (16 kb, ~90 supercoils) DNA molecules by *Vaccinia* topoisomerase I under single-turnover conditions at 22 °C. (A) Agarose gel (1 vol %) stained with ethidium bromide of the reaction of 50 nM pUC19 supercoiled DNA with 100 nM topoisomerase. In this experiment, less than 5% of the initial substrate DNA was contaminated with nicked plasmid. The photograph is overexposed and contrast enhanced so that the low levels of topoisomer intermediates can be visualized. The supercoiled substrate and overlapping early intermediates [S (+I)], late intermediates (I), and product bands (P) are indicated. As expected, the relaxed products migrate as positively supercoiled bands in this electrophoresis buffer because the ionic strength is less than that used in the relaxation reaction (Anderson & Bauer, 1978). In this gel, resolved intermediates are easily distinguished from products because, by definition, they appear and subsequently disappear with time. (C, upper panel) Plot of the time dependence of the change in the apparent mobility of the supercoiled substrate band due to partial overlap with early topoisomer intermediates which have slightly different mobilities than the initial population of supercoiled substrate molecules (see panel A and Experimental Procedures). This mobility change, which shows a first-order dependence with respect to time (solid curve), was used to determine the fraction of unreacted substrate at each time point (see Experimental Procedures). The validity of this convenient method was established by the experiment shown in panel B, in which the substrate topoisomers were completely resolved from all intermediates and products by performing electrophoresis in the presence of 25 μg/mL chloroquine diphosphate. In this chloroquine-containing gel, the substrate as well as intermediates and product are positively supercoiled. (C, lower panel) Plot of the time dependence of the concentrations of supercoiled substrate calculated using the mobility shifts (closed triangles), substrate determined from direct measurement using the chloroquine gel (asterisks), all topoisomer intermediates (open diamonds), and relaxed products (open triangles). The curves were generated by simulation using the mechanism shown in Figure 2B; the optimized kinetic parameters are reported in Table 1. The right lane for the gel shown in the upper panel ($t = 60$ s) was not quantitated due to the unreliable response of the imaging device for the lane on the extreme right edge of the gel. (D) Ethidium bromide-stained 0.6 vol % agarose gel of the reaction of 40 nM pHINDF supercoiled DNA with 40 nM topoisomerase. (E, upper panel) Apparent mobility change for the pHINDF supercoiled substrate band due to overlap with early topoisomer intermediates (see above). (E, lower panel) Plot of the time dependence of the concentrations of supercoiled substrate (closed triangles), all topoisomer intermediates (open diamonds), and relaxed products (open triangles). The curve for the disappearance of the substrate is drawn using the same rate constants for cleavage and religation determined for pUC19 (Table 1). The dashed curves drawn through the data for intermediates and product were *not* derived from simulation of these data, because the relaxation of this plasmid has too many intermediates to model explicitly (see Experimental Procedures). These dashed curves are only shown to guide the eye.

equilibrium cleavage and religation, followed by rate-limiting supercoil release, because this mechanism was incompatible with the observed slow rate of substrate disappearance *and* the early formation of fully relaxed product.

Figure 5C (upper panel) shows a plot of the apparent mobility change of the supercoiled substrate as a function of time. This mobility change results from overlap of the initial population of substrate topoisomers with that of early supercoiled intermediates which have slightly different average mobilities. This effect is not an artifact of electrophoresis because (i) it is highly reproducible (even on different gel systems), (ii) it is independent of the amount of plasmid DNA loaded in each gel lane, (iii) it is observed only for the "substrate" band and *not* for the relaxed products, and (iv) the mobility shift is more pronounced for a larger plasmid that generates more partially overlapped intermediates (Figure 5D).

Table 1: Optimized Kinetic Parameters for Relaxation of Supercoiled pUC19 DNA by the *Vaccinia* Type I Topoisomerase[a]

k_{cl}	k_r	k_{sup}	Δn	i_{tot}
0.3 s^{-1}	4 s^{-1}	20 s^{-1}	5	3

[a] The kinetic parameters are defined in the text (see eqs 2, 4, 6, 8, and 9) and refer to steps in the mechanism shown in Figure 2. We estimate maximum errors of ±20% for k_{cl} and k_r and ±30% for k_{sup} and Δn.

To establish that this mobility change was due to partially overlapped early topoisomer intermediates, we performed an identical single-turnover relaxation experiment in which the quenched time points were electrophoresed on a 1% agarose gel containing 25 μg/mL chloroquine diphosphate. In this gel system (Figure 5B), the substrate topoisomers (which are positively supercoiled under the electrophoresis conditions) are fully resolved from *all* intermediates and product. Therefore, the fractional amount of substrate at each time point could be *directly* measured and compared with that calculated from the mobility shift method. The substrate concentrations that were determined using this analysis (asterisks, Figure 5C) were indistinguishable within experimental error from those calculated using eq 1 (compare filled triangles with asterisks in Figure 5C, lower panel). These results establish the validity and accuracy of the convenient mobility shift method.

Interestingly, the mobility change follows a first-order time course that is indistinguishable from that of strand cleavage (Table 1). In other words, the cleavage step appears to be rate-limiting for formation of intermediates. This result provides additional evidence in support of the previous conclusion (Stivers et al., 1994a) which holds that the overall rate-limiting step in single-turnover supercoil relaxation is the strand cleavage event.

Control experiments demonstrated that the reaction was zero-order in substrate and enzyme when both were kept at equimolar concentrations of $\geq$35 nM. It is important to point out that the interpretation of these results is not influenced by whether the enzyme remains bound to a single DNA molecule during the single-turnover reaction or acts distributively, because the enzyme is saturated with DNA, and the binding and release steps (if occurring) must be fast relative to the rate-limiting cleavage step. Furthermore, the mechanism of relaxation is not significantly biased by multiple enzyme molecules cleaving the DNA, because kinetic results indistinguishable from those shown in Figure 5A were obtained using [E]/[DNA] ratios of 1/1, 1/2, and 1/3. This kinetic result is entirely consistent with the single major cleavage site detected in the equilibrium measurements above (Figure 3).

Three predictions that follow from this kinetic analysis are that a larger plasmid with more supercoils than pUC19 should show (i) the same rate of substrate disappearance, (ii) a greater accumulation of intermediates, and (iii) a decreased rate of product formation. These predictions are based on eqs 2, 3, and 9, respectively, which show that the initial cleavage rate is independent of the size of the substrate and that the total transit time for appearance of product ($1/k_{relax}$), and the number of intermediate pools that are generated (i_{tot}), are proportional to the number of initial supercoils in the substrate. Furthermore, a plot of the ratio of product to intermediate concentrations ([P]/[I]) as a function of time for the larger plasmid should show a slope in the steady state that is smaller than that for pUC19 (see Figure 4D).

To test these predictions, we examined the relaxation of the larger plasmid pHINDF which has 6-fold more supercoils than pUC19 (Figure 5D). Although the relaxation of this plasmid generates far too many intermediates to simulate explicitly (see Experimental Procedures), the following observations are in accord with each of the three predictions listed above. First, the observed rate of disappearance of supercoiled substrate is unchanged from that of pUC19 (compare the lower portions of panels C and E of Figure 5, noting the different time scales). Second, the amounts of intermediates formed at early time points are about 4-fold greater than that seen with pUC19. Third, the amount of product formed at early time points is less than that seen with pUC19. Consistent with these observations, a plot of the [P]/[I] ratio as a function of time for the reaction of pHINDF shows a slope in the steady-state region that is about 5-fold smaller than that for pUC19 (see the dashed line in Figure 6). In addition, the mobility change of the band corresponding to the supercoiled substrate and overlapping early intermediates also follows an exponential time course equivalent to the cleavage rate (upper panel, Figure 5E). Taken together, these results provide strong support for the applicability of the same free rotation kinetic mechanism in describing the reactions of both the small and large supercoiled plasmids.

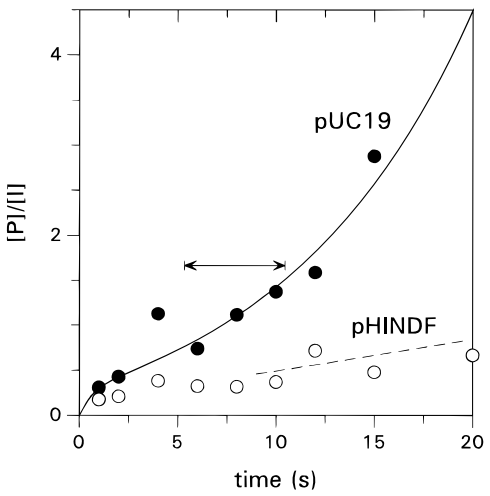

FIGURE 6: Plot of the product to intermediate ratio ([P]/[I]) against time for the relaxation of supercoiled pUC19 (closed circles) and pHINDF DNA (open circles). The solid line drawn through the pUC19 data is the theoretical curve obtained from the mechanism of Figure 2B using the kinetic parameters in Table 1. The dashed line through the pHINDF data is a best-fit line to the linear region of the time course (i.e. where the intermediates are in a steady state) and has a slope 4−6-fold smaller than the steady-state region of the pUC19 data (indicated by the arrow).

Mechanistic Implications. These kinetic results are significant because a proposed role for type I topoisomerases is removal of supercoils that are generated during transcription and replication by RNA and DNA polymerases (Wang, 1991). For instance, the *Vaccinia* DNA polymerase incorporates nucleotides at a rate of about 30 nucleotides/s *in vitro*, which indicates that at least three supercoils per second are generated at the replication fork *in vivo* (McDonald & Traktman, 1994). If a strand passage mechanism were followed, the topoisomerase reaction would be limited by the strand cleavage rate of 0.3 s^{-1}, which is 10-fold slower than the rate of supercoil generation. If one assumes a minimum stoichiometry of one topoisomerase molecule per replication fork, then this disparity between the rates of supercoil generation and removal at the replication fork would eventually hinder the rate of replication. Thus, the average rate of supercoil release $k_{sup}/\Delta n$ (=4 s^{-1}) (where k_{sup} = 20 s^{-1} and Δn = 5) provides a single topoisomerase enzyme with a mechanism for removing supercoils as fast as they are generated during these polymerization processes (3 s^{-1}), even though the rate of strand cleavage is only 0.3 s^{-1}. Of course, the capacity for removal of supercoils at

the replication fork would be even greater if more than one topoisomerase is involved in the replication process.

Another question concerning the reactivity of type I topoisomerases is whether these enzymes maintain a steady-state superhelical density in cellular DNA by modulating their reactivity in accord with the topological state of DNA (i.e. are the enzymes less active on DNA with lower superhelical density?). The results reported here and previously for the *Vaccinia* enzyme show that there is little difference between the cleavage equilibrium constants for linear and supercoiled DNA and a ≤4-fold difference between the cleavage and religation rates between these substrates (Stivers et al., 1994a,b).[5] Thus, there is no significant preference for supercoiled substrates in the chemical steps of the reaction. A similar conclusion which holds that the catalytic constants for the topoisomerization reaction are not topology-dependent has been previously inferred for the type I enzymes isolated from wheat germ, calf thymus, and yeast (Caserta et al., 1990; Camilloni et al., 1989). However, in these indirect studies, the individual rate constants were not measured, and the conclusions were based on the relative extents of cleavage of supercoiled and relaxed substrates in the presence of the drug camptothecin or, alternatively, by the competitive inhibition of the relaxation of a supercoiled substrate by linear and relaxed DNA molecules. Hence, it may be that these eukaryotic enzymes follow the same free rotation mechanism established here for the *Vaccinia* type I topoisomerase.

The value for k_{sup} of 20 s^{-1} measured here may represent a *lower limit estimate* for the spontaneous rate of unwinding of nicked supercoiled plasmid DNA because the enzyme has been shown to make noncovalent contacts with the duplex DNA downstream from the site of strand cleavage, and these interactions may influence the rate and processivity of the supercoil release step (Sekiguchi & Shuman, 1994b). We feel that it is unlikely that the enzyme actively *accelerates* supercoil unwinding, which is apparently a stochastic process governed only by the relative rates of religation and DNA strand rotation.

In contrast with the equivalent rate constants observed with supercoiled and relaxed DNA substrates for cleavage and for religation, there appears to be a large difference in the reactivity of these substrates in the binding step. This conclusion is suggested because the single-turnover reactions with supercoiled substrates were found to be independent of enzyme or DNA concentrations using conditions where small oligonucleotide substrates are not quantitatively bound by the enzyme.[6] This difference may be due to a different intrinsic affinity of the enzyme for supercoiled substrates as compared to linear molecules (Stivers et al., 1994a), or simply the greater concentration of binding sites in the larger plasmid molecule. Because the enzyme shows, at most, a 10-fold discrimination for binding its cognate site over nonspecific DNA (Sekiguchi & Shuman, 1994b), it is possible that the mechanism for finding the specific catalytic site involves binding to noncognate sites in the DNA followed by linear diffusion along the DNA. Such a mechanism would explain the observed differences at the binding step seen for small oligonucleotides and supercoiled DNA.

On the basis of structural and biochemical studies, it has been postulated that the type II topoisomerase from yeast actively transports a duplex DNA segment through the cleaved DNA duplex and that this process is coupled to ATP binding and hydrolysis (Lindsley & Wang, 1993; Berger et al., 1996). Indeed, the comparable data of Lindsley and Wang (1993) show that the relaxation of pBluescript DNA (2950 bp) by the yeast type II enzyme occurs with the formation of a significant number of intermediates prior to the appearance of fully relaxed product, as would be expected for a coupled strand passage mechanism. Using an analytical method different from that employed here, a rate constant for DNA transport of 0.73 s^{-1} at 17.5 °C was measured for the yeast enzyme. This transport rate is comparable to the rate constants for cleavage and religation reported here for the *Vaccinia* type I enzyme and suggests that the strand passage rate is more tightly coupled to, and perhaps limited by, the chemical steps of the reaction. This result suggests that, in general, the eukaryotic type I topoisomerases may follow a different mechanism for supercoil release than the ATP-dependent type II enzymes.

The free rotation mechanism observed for the *Vaccinia* enzyme also suggests a mechanism for the DNA catenation reaction catalyzed by the eukaryotic type I enzymes (McCoubrey & Champoux, 1986; Holden & Low, 1985). Since these catenation reactions require a pre-existing single-strand nick in the DNA, it seems likely that a *passive* catenation mechanism is followed. In this mechanism, a transient linear DNA intermediate is first generated by topoisomerase cleavage of the DNA opposite to the pre-existing nick. A second circular DNA molecule is then trapped by religation of the linearized DNA, resulting in two fully catenated circles. This catenation mechanism suggests that the enzyme does not form strong noncovalent interactions with the DNA 3′ to the cleavage site, thereby allowing the DNA end to diffuse from the enzyme active site. Indeed, this suggestion is supported by the observation that, with linear DNA substrates, 3′ segments of the cleaved strand readily dissociate from the enzyme after the cleavage event (Shuman, 1991).

Conclusions. We have shown that the *Vaccinia* type I topoisomerase follows a free rotation mechanism for removing supercoils from DNA, with an average (Δn) of five supercoils removed per cleavage event. This mechanism allows the enzyme to efficiently remove supercoils from DNA even though the chemical step of cleavage is ~10-fold slower than the average rate of supercoil release

[5] We previously reported rate constants for single-turnover cleavage and religation in the range of 0.06−0.09 and 0.7−1 s^{-1}, respectively, for small linear duplex substrates in which the leaving strand for the cleavage reaction was a dinucleotide and the entering strand for the religation reaction was an 8-mer strand (Stivers et al., 1994a,b). Subsequently, we have found a modest dependence of the cleavage rate on the length of the leaving strand, with a 4-mer and 6-mer strand being cleaved with a rate constant of 0.11 s^{-1} (J. T. Stivers, unpublished results, 1995) and 0.28 s^{-1}, respectively (S. Shuman, personal communication, 1996). The latter value is indistinguishable from that measured here for a supercoiled substrate.

[6] We have previously measured a dissociation constant of 54 nM for the enzyme from a 25/25-mer oligonucleotide in 50 mM Tris-HCl at 20 °C (Stivers et al., 1994a). We also found a 10-fold increase in the dissociation rate constant when the binding reaction mixture was supplemented with 5 mM $MgCl_2$, suggesting that the binding constant is even *weaker* under conditions used for the relaxation reactions (i.e. when divalent and monovalent cations are present). A similar K_d value of ~25 nM can be estimated from the data of Sekiguchi and Shuman (1994) for the noncovalent binding of the Y274F mutant to a 24/24-mer oligonucleotide in 50 mM Tris-HCl at 37 °C. A lower apparent K_d value for binding to pUC19 is required to explain the observed zero-order kinetics of supercoil relaxation.

($k_{sup}/\Delta n = 4\ s^{-1}$). This free rotation mechanism for a type I topoisomerase differs from that proposed for the yeast type II enzyme (Lindsley & Wang, 1993), which apparently follows a strand passage mechanism for supercoil release.

The general model we have employed for analysis of supercoil relaxation should be applicable to other type I and type II topoisomerase-catalyzed reactions provided that (i) appropriate single-turnover conditions can be achieved and (ii) the required number of intermediates can be modeled. The method works best for a free rotation type mechanism, using a moderately sized plasmid such as pUC19, when the average number of supercoils removed per cleavage event yields a total number of intermediate pools of four or fewer. Accordingly, a smaller plasmid substrate with fewer supercoils would be optimal for modeling a strand passage mechanism, because of the accumulation of more intermediates during this process. Nevertheless, we have shown by simulation that a simple comparison of the [product]/[intermediate] ratio as a function of the fraction of substrate reacted (Figure 4C) can distinguish between the two limiting mechanisms for supercoil release.

ACKNOWLEDGMENT

We thank Dr. Roger McMacken at the Department of Biochemistry at The Johns Hopkins University School of Hygiene and Public Health for permission to use the imaging equipment and Drs. JoAnn Sekiguchi and Stewart Shuman for helpful discussions and for providing us with purified topoisomerase and the plasmid pHINDF.

SUPPORTING INFORMATION AVAILABLE

Detailed protocol for simulating the relaxation of pUC19 supercoiled DNA and a summary table (3 pages). Ordering information is given on any current masthead page.

REFERENCES

Anderson, K. S., Sikorski, J. A., & Johnson, K. A. (1988) *Biochemistry 27*, 7395−7406.
Anderson, P., & Bauer, W. (1978) *Biochemistry 17*, 594−601.
Barshop, B. A., Wrenn, R. F., & Freiden, C. (1983) *Anal. Biochem. 130*, 134−145.
Berger, J. M., Gamblin, S. J., Harrison, S. C., & Wang, J. C. (1996) *Nature 379*, 225−232.
Camilloni, G., Di Martino, E., Di Mauro, E., & Caserta, M. (1989) *Proc. Natl. Acad. Sci. U.S.A. 86*, 3080−3084.
Caserta, M., Amadei, A., Camilloni, G., & Di Mauro, E. (1990) *Biochemistry 29*, 8152−8157.
Champoux, J. J. (1990) in *DNA Topology and its Biological Effects* (Cozzarelli, N. R., & Wang, J. C., Eds.) pp 217−242, Cold Spring Harbor Laboratory Press, Plainview, NY.
Espejo, R. T., & Lebowitz, J. (1976) *Anal. Biochem. 72*, 95−103.
Fersht, A. R. (1985) *Enzyme Structure and Mechanism*, 2nd ed., pp 117−118, W. H. Freeman & Co., New York.
Gellert, M. (1981) *Annu. Rev. Biochem. 50*, 879−910.
Holden, J. A., & Low, R. L. (1985) *J. Biol. Chem. 260*, 14491−14497.
Keller, W. (1975) *Proc. Natl. Acad. Sci. U.S.A. 72*, 4876−4880.
Lindsley, J., & Wang, J. C. (1993) *J. Biol. Chem. 268*, 8096−8104.
Liu, L. F., & Wang, J. C. (1991) *DNA Topoisomerases in Cancer* (Potmesil, M., & Kohn, K. W., Eds.) pp 13−22, Oxford University Press, New York.
McCoubrey, W. K., Jr., & Champoux, J. J. (1986) *J. Biol. Chem. 261*, 5130−5137.
McDonald, W. F., & Traktman, P. (1994) *J. Biol. Chem. 269*, 31190−31197.
Morham, S. G., & Shuman, S. (1992) *J. Biol. Chem. 267*, 15984−15992.
Sekiguchi, J., & Shuman, S. (1994a) *J. Biol. Chem. 270*, 31731−31734.
Sekiguchi, J., & Shuman, S. (1994b) *Nucleic Acids Res. 22*, 5360−5365.
Sekiguchi, J., & Shuman, S. (1995) *J. Biol. Chem. 270*, 11636−11645.
Sekiguchi, J., & Shuman, S. (1996) *J. Biol. Chem. 271*, 19436−19442.
Shuman, S. (1991) *J. Biol. Chem. 266*, 1796−1803.
Shuman, S. (1992) *J. Biol. Chem. 267*, 8620−8627.
Shuman, S., & Moss, B. (1987) *Proc. Natl. Acad. Sci. U.S.A. 86*, 3489−3493.
Shuman, S., & Prescott, J. (1990) *J. Biol. Chem. 265*, 17826−17836.
Shuman, S., Golder, M., & Moss, B. (1989) *Virology 170*, 302−306.
Stivers, J. T., Shuman, S., & Mildvan, A. S. (1994a) *Biochemistry 33*, 327−339.
Stivers, J. T., Shuman, S., & Mildvan, A. S. (1994b) *Biochemistry 33*, 15449−15458.
Svejstrup, J. Q., Christiansen, K., Andersen, A. H., Lund, K., & Westergaard, O. (1990) *J. Biol. Chem. 265*, 12529−12535.
Wang, J. (1991) *J. Biol. Chem. 266*, 6659−6662.

BI962880T